Silicon Fibre Devices for Nonlinear Applications

A. C. Peacock,[1] P. Mehta,[1] L. Shen,[1] F. H. Suhailin,[1,2] N. Vukovic,[1] and N. Healy[1]
[1] Optoelectronics Research Centre, University of Southampton, Southampton SO17 1BJ, United Kingdom
[2] School of Fundamental Science, Universiti Malaysia Terengganu, 21300 Kuala Terengganu, Malaysia

Paper Summary

We review our progress in the development of nonlinear devices from the silicon optical fibre platform. The nonlinear performance will be benchmarked through demonstrations of high speed all-optical wavelength conversion, modulation, and continuum generation.

Introduction

Silicon waveguides are an ideal platform for nonlinear optical signal processing due to their large Kerr nonlinearity and high silicon-core/silica-cladding index contrast which allows for tight mode confinement. As such, a number of all-optical nonlinear devices have been demonstrated using rectilinear silicon waveguides on-chip including optical regeneration, modulation, and switching. The incorporation of silicon into the optical fibre geometry provides an important step towards integrating semiconductor functionality with conventional fibre infrastructures [1]. In this paper we review our progress in the development of nonlinear devices from the silicon optical fibre platform. Although typical core sizes for our fibres are on the order of a few microns, by exploiting the high nonlinearity of the hydrogenated amorphous silicon (a-Si:H) material we have been able to perform the first characterization of the nonlinear transmission properties of this new class of fibre, with subsequent demonstrations of ultrafast wavelength conversion, modulation, and continuum generation [2]. The results illustrate the potential for these fibres to find use in wide ranging applications from signal processing to biosensing and spectroscopy.

Nonlinear Characterization

The silicon core fibres are fabricated using a high pressure chemical deposition technique. This technique can be easily adapted to fill capillaries with a range of inner diameters, as well as microstructured or tapered templates, so that the waveguiding properties can be optimized for specific applications [2]. Fig. 1 shows examples of the silicon core fibres used for the nonlinear investigations, where (a) shows two a-Si:H core fibres of differing diameters and (b) shows a tapered polysilicon (p-Si) core fibre. As of to date, the lowest optical losses that have been measured for these core materials at the telecoms wavelength of 1.54μm are ~0.8dB/cm for a-Si:H (~0.3dB/cm at 2.7μm) [3], and 5dB/cm for p-Si [4], comparable to those measured on-chip.

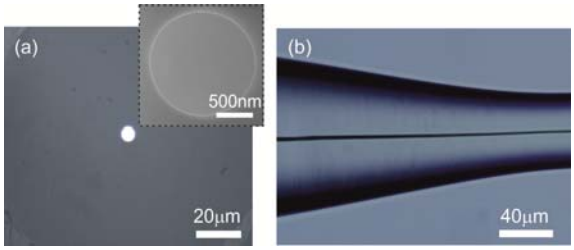

Figure 1 (a) Microscope image of a a-Si:H fibre with a 6μm core (inset, SEM of a 2μm core fibre). (b) Tapered p-Si core fibre.

Nonlinear propagation in the silicon fibres can be described by a modified form of the nonlinear Schrödinger equation (NLSE), together with a coupled equation for the free carrier density N_c [2]:

$$\frac{\partial A}{\partial z} = -\frac{i\beta_2}{2}\frac{\partial^2 A}{\partial t^2} + i\gamma|A|^2A - \frac{1}{2}(\sigma_f + \alpha_l)A,$$

$$\frac{\partial N_c}{\partial t} = \frac{\beta_{\mathrm{TPA}}}{2h\nu_0}\frac{|A|^4}{A_{\mathrm{eff}}^2} - \frac{N_c}{\tau_c}.$$

Here A is the pulse envelope, α_l is the linear loss, β_2 is the group velocity dispersion, and the complex nonlinearity parameter is defined as: $\gamma = k_0 n_2/A_{\mathrm{eff}} + i\beta_{\mathrm{TPA}}/2A_{\mathrm{eff}}$ in terms of the Kerr n_2 and two-photon absorption (TPA) β_{TPA} coefficients, as well as the mode area A_{eff}. The free carrier (FC) contribution is described by: $\sigma_f = \sigma(1 + i\mu)N_c$ (absorption σ and dispersion μ) and τ_c is the carrier lifetime. Using this form of the NLSE, we have determined the nonlinear parameters for the a-Si:H core fibres at 1.54μm to be in the range: n_2 =1.5–1.8×10^{-13}cm^2/W and β_{TPA} =0.5–0.8cm/GW, which yields a nonlinear figure of merit $\mathrm{FOM_{NL}} = n_2/\beta_{\mathrm{TPA}}\lambda \sim 1.5 - 2$ [5], considerably larger than that for the single crystal material [6]. More recently, by extending our characterization beyond the telecoms window and into the short-wave infrared regime we have shown that the a-Si:H material can exhibit an even higher $\mathrm{FOM_{NL}}$ (>20) as the n_2 remains large while β_{TPA} reduces substantially as the pump wavelength moves across the TPA edge [3]. Fig. 2 shows broadband spectral generation in the a-Si:H core fibres both in the telecoms and short-wave regions. Fig. 2(a) is for a 6μm core fibre pumped at 1.54μm where the broadening is limited to ~100nm by both the strong TPA and the relatively large core size. By reducing the core size to 2μm, similar broadening can be obtained at this wavelength, albeit at a much lower peak power P_p~20W.

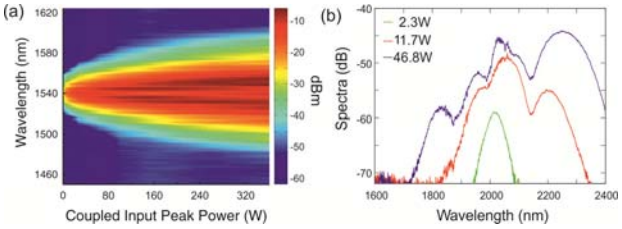

Figure 2 (a) Spectral broadening in a 6μm core a-Si:H fibre in the telecoms band. (b) Continuum generation in a 2μm core a-Si:H fibre in the short-wave infrared.

However, by shifting the pump to 2.05μm, beyond the TPA edge, Fig. 2(b) shows that broadening of up to ~700nm can be obtained in the small core fibre over a 20dB scale, comparable to the continuum generation obtained in nanoscale waveguides on-chip [7]. We note that the spectral broadening in Fig. 2(b) is also facilitated by pumping near the zero dispersion wavelength (λ_D~2.1μm) for the 2μm core fibre, with phase-matched four-wave mixing clearly observable when pumping at 2.2μm in the anomalous dispersion regime.

Ultrafast Wavelength Conversion and Modulation

As a means to exploit the large nonlinear parameters and demonstrate device functionality we have conducted a series of simple pump-probe experiments, from which the performance of the fibres can be benchmarked for all-optical processing. Fig. 3(a) shows a spectrogram of a probe pulse centred at 1.59μm (T_{fwhm}~800fs) under the influence of cross-phase modulation (XPM) induced by a strong pump pulse at 1.54μm (T_{fwhm}~750fs) for different delays [8]. From this it is clear that when the probe propagates alone (large delays) the spectral components are unaltered, whilst in the presence of the pump the peak spectral wavelength, shown by the white dashed line, is red (blue) shifted for positive (negative) delays. The asymmetry in the wavelength conversion is due to TPA at these telecoms wavelengths and could be reduced by moving either to longer wavelengths or shorter pulse durations. Nevertheless, the large 10nm red shift is sufficient to yield an extinction ratio of 12dB, suitable for use in ultrafast switching applications.

Alternatively, it is possible to make use of the large nonlinear losses for high speed all-optical cross-absorption modulation (XAM). In this process the losses induced by a strong pulsed pump can be used to imprint a dark pulse on a weak signal. Fig. 3(b) shows the absorption on a probe at 1.57μm due to a T_{fwhm}~750fs pump pulse at 1.54μm, as a function of delay. The results clearly show the ultrafast response due to TPA (~1ps), followed by a rapid recovery via carrier relaxation and then the slower recombination due to the free carriers, in agreement with a fit obtained from the coupled NLSEs [9]. The modulation yields an extinction of ~4dB, comparable to many silicon modulators, though this could be further improved by moving to shorter wavelengths where the TPA parameter is larger. By reducing the fibre core size to decrease the carrier recovery time, this modulation scheme should be capable of operating at the high bit rates necessary for communications applications.

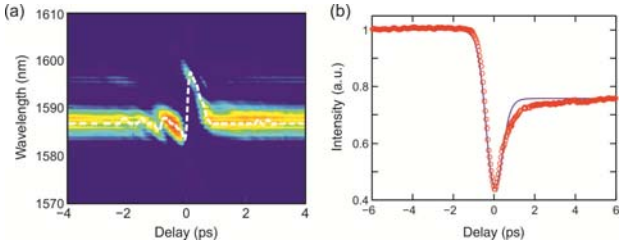

Figure 3 (a) Spectrogram of XPM induced on a probe at 1.59μm by a pump at 1.54μm (dashed white line is peak spectral wavelength). (b) XAM induced on a probe at 1.57μm by a pump at 1.54μm.

Silicon Fibre Micro Structures

A unique advantage of the silicon fibre platform is that it is possible to use standard fibre post-processing techniques to realize novel device geometries. The ability to tune the device dimensions to manipulate the light confinement in these micro-scale devices is of particular interest for low power, high speed nonlinear optical processing. For example, we have shown that by tapering the silicon core fibres, as in Fig. 1(b), it is possible to exploit the longitudinally varying dispersion and nonlinearity for nonlinear pulse shaping. Specifically, in the anomalous dispersion regime a decreasing dispersion can be used to support soliton propagation and compression, of interest to high data-rate systems [10], whilst in the normal dispersion regime it can be used to generate the linearly chirped parabolic pulses of use for regeneration and optical retiming [11]. Importantly, this nonlinear pulse shaping occurs for peak powers of only a few tens of watts compared to the kilowatt levels required for femtosecond pulses in silica fibres.

However, to further reduce the power thresholds in the fibre platform we have also shown that it is possible to fabricate silicon fibre-based microresonators. Whispering gallery mode (WGM) resonators with high quality factors (Q) and small mode volumes are becoming increasingly popular for nonlinear applications, and the large n_2 and tight mode confinement in the silicon structures greatly enhances the nonlinear effects compared to their silica fibre counterparts [12]. The silicon microresonators are formed by etching the silica cladding away from the a-Si:H core fibres, as shown in the inset of Fig. 4(a). A typical resonator transmission spectrum, as coupled via a tapered silica fibre, is plotted in Fig. 4(a) showing the sharp resonances associated with the WGMs. For a material loss of 1.5dB/cm at 1.54μm the bandwidths of the resonance dips are $\Delta\lambda$~0.1nm, corresponding to loaded Q factors of $Q_l \sim 1-2\times10^4$ [13]. By characterizing the nonlinear effects in a resonator with a

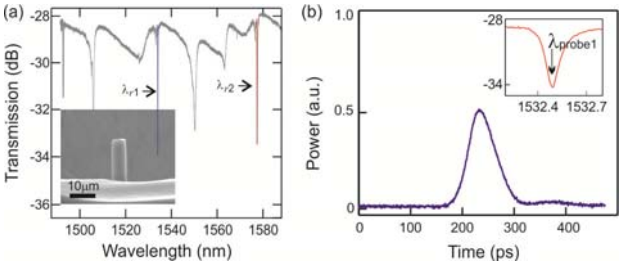

Figure 4 (a) Resonator transmission spectrum; inset is an SEM image of the etched a-Si:H microcylindrical resonator. (b) Modulated bright pulse showing on-off switching on a picosecond time scale; inset shows the probe position with respect to the cold cavity resonance dip.

6μm diameter, we have measured large Kerr resonance wavelength shifts of ~3nm when pumping with short pump pulses of only P_{ave}~20μW (P_p~ 20mW), compared to ~0.5nm shifts obtained for the thermal nonlinearity. These large Kerr shifts occur on an ultrafast time scale so that they can be readily exploited for all-optical processing using a pump-probe configuration, where a pulsed pump (positioned at λ_2) is used to modulate a CW signal coupled into an adjacent resonance (λ_1). Fig. 4(b) shows the response function of the filtered probe when the light is initially coupled on resonance so that the presence of the pump causes it to be switched on (see inset). We note that the effect of the filter on the bandwidth limited detection system is to expand the time scale and in fact the on-off switching time is on the order of ~25ps, as determined by the bandwidth of the resonator. Significantly, the optical modulation was realized at switching thresholds as low as ~5μW (P_p~5mW), with the estimated pulse energy of only 0.3pJ, almost two orders of magnitude lower in comparison to the crystalline silicon based ring resonators [14].

Conclusions

The nonlinear transmission properties of various silicon core fibre devices have been characterized and demonstrated for use in wavelength conversion, modulation, and continuum generation schemes. The ability to integrate the highly nonlinear a-Si:H material into the geometrically standardized fibre geometry should open up new avenues for nonlinear silicon photonics.

References

1. J. Ballato et al., Opt. Fiber Technol. 16 (2010) p. 399
2. A. C. Peacock et al., Laser Photonics Rev. 8 (2014) p.53
3. L. Shen et al., Opt. Express 21 (2013) p.13075
4. N. Healy et al., Advanced Photonics Congress (SOF) (2012) STu1D.1
5. P. Mehta et al., Opt. Express 18 (2010) p.16826
6. C. Koos et al., Opt. Express 15 (2007) p.5976
7. U. U. Dave et al., Opt. Express 2 (2013) p.32032
8. P. Mehta et al., Opt. Express 20 (2012) p.26110
9. P. Mehta et al., Opt. Express 19 (2011) p.19078
10. A. C. Peacock, Opt. Lett. 35 (2010) p.3697
11. A. C. Peacock and N. Healy, Opt. Lett. 35 (2010) p.1780
12. M. Pöllinger and A. Rauschenbeutel, Opt. Express 18 (2010) p.17764
13. N. Vukovic et al., Sci. Reports 3 (2013) p.2885
14. A. Almeida et al., Nature 431 (2004) p.1081